2023 8th International Conference on
Advanced Robotics and Mechatronics
July 8-10, Sanya, China

# Design and Implementation of an Underactuated Biped Robot Prototype on Compliant Ground

Qian Zhou, Xiong Yin, Zhilong Guo, Yu Pei, Zhao Feng and Daojin Yao



*Abstract*— **Considering the influence of the actual compliant grounds on the stable walking of the underactuated robot, a prototype of the planar underactuated biped walking robot is designed in this paper, and the simulation and experiment are carried out. Firstly, a biped robot model is established, and the compliant ground is equivalent to a spring-damping system. An adaptive feedforward control strategy is adopted to realize stable underactuated walking by controlling the robot's centroid velocity. Then, according to the control strategy, a 600mm high, 5.62kg weight planar underactuated robot prototype was produced, including the mechanical structure and software system. Finally, the underactuated walking with the step size of 0.1839m is realized through simulation and robot prototype experiment. The experimental results show that the robot prototype designed in this paper can carry out underactuated walking on different compliant grounds.**

## I. INTRODUCTION

Bipedal walking has been a hot research topic because of its adaptability in an unstructured environment [1],[2]. The current research points mainly centralize on topographic changes such as slopes, stairs, and uneven terrain [3]. The researchers ignore the influence of ground compliance. However, in real environments, the ground will deform and ground compliance will affect underactuated bipedal walking. For better bipedal walking, researches on the influence of ground compliance on underactuated biped walking are necessary.

In the current researches, the influence of ground compliance on biped walking have been found. Plestan found ground compliance affects the walking stability of robot in the RABBIT simulation test [4]. Westervelt found RABBIT walks at a lower speed on the steel plate than on the concrete floor [5]. Aguilar combined with fluid static and dynamics, then discussed the walking control on compliant ground from the mechanical point of view. Yong Mao proposed an energy optimization control method with variable stiffness [6]. The Achilles biped robot is designed, which can realize stable and efficient dynamic walking under the condition of environment disturbance. Chao Li studied the dynamic walking and antidisturbance problems of underactuated biped robot by adjusting the real-time landing point of the robot [7]. Peijie Zhang applied the theory of orbit stability based on Poncarel mapping to describe the stability of periodic walking gait [8]. The dichotomy method is used to estimate the attractive domain of the gait limit cycle of the robot, which reduces the computation and improves the estimation accuracy. Yang Wang found ground compliance affects walking speed and leads to walking instability [9].

In this paper, the bipedal underactuated walking model is established on compliant ground. A prototype of an underactuated biped robot is designed and built, and the correctness of the design scheme is verified by experiments. Compared with the existing work, we have the following three contributions:

- To research on the influence of ground compliance on underactuated walking, different compliance parameters are tested in the simulation environment.
- In order to verify the effectiveness of an underactuated biped robot walking with the adaptive feedforward control strategy, an underactuated biped robot prototype was designed, and the feasibility of the scheme was verified by the robot prototype.
- The controller can adjust the robot centroid velocity through gait to realize underactuated walking in different compliant grounds.

This paper is organized as follows: the establishment of the robot-ground model on underactuated bipedal walking are given in Sec.2. The control strategy is shown in Sec.3. Robot prototype construction, walking simulation and robot prototype experiment are given in Sec.4. Conclusion is given in Sec.5.

## II. ROBOT MODEL

In the paper, the ability of the ground to deform under load is called ground compliance. The walking environment that considers the ground compliance and the actual coupling state of the robot-ground is called the compliant ground environment. The ground is compliant and modelled as the spring-damper system [10], where the stiffness of the elastic spring is denoted by $k$ and the damping of viscous damper denoted by c, as shown in Fig. 1. The robot have four freedoms($q_1$, $q_2$, $q_3$, $q_4$)，where $q_1$ is a underactuated freedom.

Let lt, lc be the robot's leg lengths, mt, mc leg masses, mk knee mass， $m_h$ hip mass. $x_{st}$, $y_{st}$, $x_{sw}$ and $y_{sw}$ are the level and vertical displacement of the support foot and swing foot. $\theta$ is the angle between the line connecting the end of the supporting foot and the hip joint and the vertical plane. $\theta$ is monotonically increasing during walking and can be used as a dummy time variable [11]. In Fig. 1 show the single support

*Resrach supported by the National Natural Science Foundation of China under Grant 52005182 and 52165069, Natural Science Foundation of Jiangxi Province under Grant 20224BAB214051,Graduate Innovation Special Fund Project under Grant YC2021-S452, and by Key R & D plan of Jiangxi Province under Grant 20212BBE51010.

Qian Zhou, Xiong Yin， Zhilong Guo and Yu Pei are with the Department of Electrical and Automation Engineering,East China Jiaotong University. (e-mail: zhouh@ecjtu.edu.cn; hero@ecjtu.edu.cn; guozhilong202202@163.com; 2020028085800020@ecjtu.edu.cn).

Zhao Feng is with the faculty of the School of Power and Mechanical Engineering, Wuhan University. (e-mail: fengzhao@whu.edu.cn).

Daojin Yao is with the faculty of the Department of Electrical and Automation Engineering, East China Jiaotong University. (corresponding author to provide phone: 87046402; e-mail: ydaojin@whu.edu.cn).

phase (SSP) and the double support phase (DSP) of the robot walking.

Compared to walking on rigid ground, the contact phase on compliant ground is non-transient. The contact phase of the biped robot begins when the swing leg strikes the ground and ends when the stance leg lifts off the ground.

The dynamic model of the robot-ground system during SSP can be derived by using the method of Lagrange. A standard equation of motion is resulted:

$$M_{\mathrm{e}}(\boldsymbol{q}_{\mathrm{e}})\ddot{\boldsymbol{q}}_{\mathrm{e}}+H_{\mathrm{e}}(\boldsymbol{q}_{\mathrm{e}},\dot{\boldsymbol{q}}_{\mathrm{e}})=B_{\mathrm{e}}\boldsymbol{u}+B\boldsymbol{F}_{\mathrm{st}}(\boldsymbol{q}_{\mathrm{e}},\dot{\boldsymbol{q}}_{\mathrm{e}}) \tag{1}$$

$$\boldsymbol{F}_{\mathrm{st}}(\boldsymbol{q}_{\mathrm{e}},\dot{\boldsymbol{q}}_{\mathrm{e}})=\begin{bmatrix}\boldsymbol{0}_{5\times1}\\ -c_i\dot{x}_{\mathrm{st}}-k_i(x_{\mathrm{st}}-x_{\mathrm{st0}})\\ -c_i\dot{z}_{\mathrm{st}}-k_i y_{\mathrm{st}}\end{bmatrix} \tag{2}$$

The matrix $\boldsymbol{q}_{\mathrm{e}}=[q_1;q_2;q_3;q_4;x_{\mathrm{st}};y_{\mathrm{st}}]$ is the joint Angle; $M_{\mathrm{e}}(\boldsymbol{q}_{\mathrm{e}})$ is the 6×6 inertia matrix; $H_{\mathrm{e}}(\boldsymbol{q}_{\mathrm{e}},\dot{\boldsymbol{q}}_{\mathrm{e}})$ is the 6×1 Coriolis force and gravity vector; $B_{\mathrm{e}}$ is the $6\times6$ joint torque input matrix; $\boldsymbol{u}$ is the joint torque driving matrix, $B$ is the 6×6 matrix of the direction of the supporting foot force on the ground, $\boldsymbol{F}_{\mathrm{st}}(\boldsymbol{q}_{\mathrm{e}},\dot{\boldsymbol{q}}_{\mathrm{e}})$ is the force of the ground on the robot, $x_{\mathrm{st0}}$ is the initial horizontal position of the swing foot when it contacts the ground. $k_i$, $c_i$ are the ground stiffness and damping coefficient at the contact.

The dynamics model of DSP phase is as follows A standard equation of motion is

$$M_{\mathrm{e}}(\boldsymbol{q}_{\mathrm{e}})\ddot{\boldsymbol{q}}_{\mathrm{e}1}+H_{\mathrm{e}}(\boldsymbol{q}_{\mathrm{e}},\dot{\boldsymbol{q}}_{\mathrm{e}})=B_{\mathrm{e}}\boldsymbol{u}+B\boldsymbol{F}_{\mathrm{st}}(\boldsymbol{q}_{\mathrm{e}},\dot{\boldsymbol{q}}_{\mathrm{e}})+E_{\mathrm{sw}}^{T}\boldsymbol{F}_{\mathrm{sw}}(\boldsymbol{q}_{\mathrm{e}},\dot{\boldsymbol{q}}_{\mathrm{e}}), \tag{3}$$

$$\boldsymbol{F}_{\mathrm{sw}}(\boldsymbol{q}_{\mathrm{e}},\dot{\boldsymbol{q}}_{\mathrm{e}})=\begin{bmatrix}\boldsymbol{0}_{5\times1}\\ -c_j\dot{x}_{\mathrm{sw}}-k_j(x_{\mathrm{sw}}-x_{\mathrm{sw0}})\\ -c_j\dot{z}_{\mathrm{sw}}-k_j y_{\mathrm{sw}}\end{bmatrix}. \tag{4}$$

Where $M_{\mathrm{e}}(\boldsymbol{q}_{\mathrm{e}}), H_{\mathrm{e}}(\boldsymbol{q}_{\mathrm{e}},\dot{\boldsymbol{q}}_{\mathrm{e}}), B_e, B, \boldsymbol{u}$ and $\boldsymbol{F}_{\mathrm{st}}(\boldsymbol{q}_{\mathrm{e}},\dot{\boldsymbol{q}}_{\mathrm{e}})$ have the same definition as (1). $\boldsymbol{F}_{\mathrm{sw}}(\boldsymbol{q}_{\mathrm{e}},\dot{\boldsymbol{q}}_{\mathrm{e}})$ is the reaction force at the end of the swing leg, $E_{\mathrm{sw1}}$ is the Jacobian matrix at the end of the swing leg, $x_{\mathrm{sw0}}$ is the initial horizontal position of the swing foot when it contacts the ground. $k_j$, $c_j$ are the ground stiffness and damping coefficient at the contact point between the support foot and the ground.

## III. Control Strategy

### A. Adaptive Control

Based on the observation of human walking characteristics, an adaptive feedforward control strategy is proposed in this paper. By controlling the robot's centroid speed in a stable walking range, the biped robot can achieve periodic stable walking [12].

The control strategy selects the horizontal distance of centroid movement in a complete walking cycle $x_{\mathrm{f}}$ as the control input, and the horizontal speed of centroid $u_{\mathrm{f}}$ at the end of the cycle as the control output. The robot control system is simplified into a single input-single output system. The control strategy ensures the tracking of the ideal $u_{\mathrm{fd}}$ by adjusting the $x_{\mathrm{fc}}$ in the walking process of the biped robot and realizes the stable walking. This is shown in Fig. 2.

### B. Virtual Beam

Virtual constraint method is an effective control method to realize underactuated stable walking of bipedal [13]. Its essence is to design a full constraint form throughout the whole gait cycle, and apply the full constraint to the robot. The joint Angle error under the constraint is used as the output, and the joint Angle tracking is realized by ensuring that the output is always zero [14].

In order to reduce the space dimension of the system, Rouse's protocol is used to select the monotonically increasing quantity in the walking cycle instead of the actual time coordinate [15]. In this paper, $q_1$ is used as the reference quantity of the walking cycle of the robot, and the active joint constraint equation is

$$e=h(\boldsymbol{q}_{\mathrm{e}})=q_a-q_{\mathrm{d}}(q_1). \tag{5}$$

Let $\boldsymbol{u}_1^*$ be the ideal actuation input of the joint, considering (4), the control torque is

$$\boldsymbol{u}_1^*=\left[\frac{\partial h(\boldsymbol{q}_{\mathrm{e}})}{\partial \boldsymbol{q}_{\mathrm{e}}}M_{\mathrm{e}}^{-1}(\boldsymbol{q}_{\mathrm{e}})B_{\mathrm{e}}\right]^{-1}\cdot\left[\frac{\partial^2 h(\boldsymbol{q}_{\mathrm{e}})}{\partial \boldsymbol{q}_{\mathrm{e}}^{2}}\dot{\boldsymbol{q}}_{\mathrm{e}}^{2}(t)+\frac{\partial h(\boldsymbol{q}_{\mathrm{e}})}{\partial \boldsymbol{q}_{\mathrm{e}}}M_{\mathrm{e}}^{-1}(\boldsymbol{q}_{\mathrm{e}})H(\boldsymbol{q}_{\mathrm{e}},\dot{\boldsymbol{q}}_{\mathrm{e}})\right]. \tag{6}$$

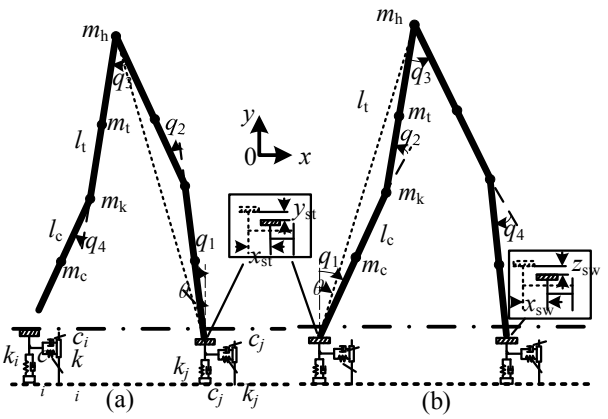


Figure 1. *Robot walking process on compliant ground*

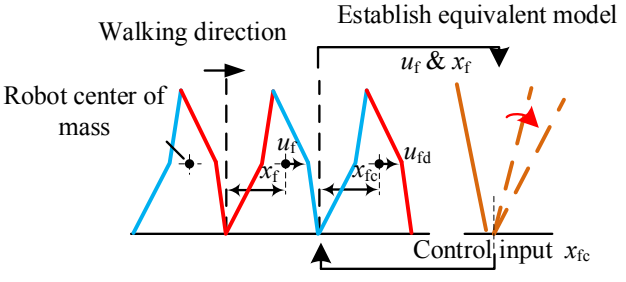


Figure 2. *The schematic diagram of adaptive feedforward control strategy*

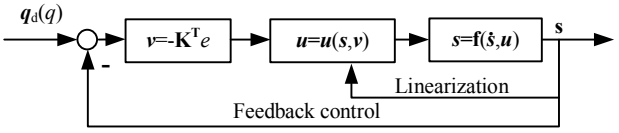


Figure 3. *Schematic diagram of feedback linearization control*

Due to the difference between the ideal robot model and the actual prototype, the ideal torque $\boldsymbol{u}_1^*$ needs to be corrected.

In this paper, the feedback linearization method is used, and its working principle is shown in Fig. 3. The control includes two links: the feedback control loop and the linearization loop [16]. Firstly, the torque $\boldsymbol{v}$ was calculated through the feedback of the actual state $\boldsymbol{s}$ and the ideal joint trajectory $q_d(q_1)$. Then, the linearization loop was applied to modify the torque $\boldsymbol{v}$ to obtain the control torque $\boldsymbol{u}$. Finally, the torque is input into the system, and the controller collects the system state and repeats the feedback control loop.

Through the feedback control parameters $K_p$ and $K_d$, the active control torque is modified so that the active joint pose of the robot in the SSP always converges to the reference input.

### C. Bezier

In order to realize underactuated walking, the motion trajectories of the active control joints $q_2$, $q_3$ and $q_4$ of the robot are planned. Based on Poincare regression mapping method, the third order Bayes curve difference is used to generate the robot joint motion trajectory [17]. Using $q_1$ as a reference quantity, the joint motion trajectory is planned. Suppose that the initial and terminal states of the robot walking are $[\,q_i\,,\dot{q}_i\,]^T$ and $[\,q_f\,,\dot{q}_f\,]^T$. The motion trajectory of each joint of the robot is $q_a$:

$$\begin{cases} q_i = \left[q_{1i}, q_{2i}, q_{3i}, q_{4i}\right]' \\ q_f = \left[q_{1f}, q_{2f}, q_{3f}, q_{4f}\right]' \\ q_a(q_1) = \sum_{k=0}^{3} a_k \dfrac{3!}{k!(3-k)!} s^k (1-s)^{3-k} \\ s = \dfrac{q_1 - q_{1f}}{q_{1f} - q_{1i}} \end{cases} . \tag{7}$$

The coefficients are as follows:

$$\begin{cases} a_0 = (q_i)_a \\ a_1 = (q_i)_a + \dfrac{q_{1f} - q_{1i}}{3} \dfrac{\partial q_a}{\partial q_1}(q_{1i}) \\ a_2 = (q_f)_a + \dfrac{q_{1f} - q_{1i}}{3} \dfrac{\partial q_a}{\partial q_1}(q_{1f}) \\ a_3 = (q_f)_a \end{cases} , \tag{8}$$

where $(.)a$ represents the active control joint， $a = 2,3,4$.

## IV. Simulation and Experiment

In order to verify the control method in this paper, a simulation environment was constructed, numerical simulation was carried out, and an experimental platform for underactuated robot walking was built to verify the rationality of the scheme.

### A. Physical Prototype

An experimental platform for underactuated bipedal walking was designed to verify the effectiveness of the control strategy in this paper. The prototype consisted of two parts: mechanical structure and control system [18]. The robot adopts a four-bar structure with one hip joint and two knee joints, among center-of-mass speed by adjusting walking. Therefore, the prototype control system must be able to detect the robot's state in real time and adjust its moving gait online. The prototype control system includes two parts: hardware and software.

In this paper, the experimental platform used is composed of robot body and motion cage. The total mass of the robot body is 5.62kg. The robot has 1 hip joint and 2 knee joints, with a total of 3 active degrees of freedom. The hip joint is controlled by two motors, and the distance from the hip joint to the sole of the foot is 600mm. The motion cage is 1050mm long, 450mm wide, 650mm high, and weighs 5.8kg. The prototype is shown in Fig. 4.

The motion cage is equipped with a directional wheel at the lower end. Detailed parameters of each part of the prototype are shown in Table I.

The control system is the core of the prototype to realize underactuated walking. In order to shorten the development cycle, this paper builds the platform control system, devices are shown in Table I and Table II.

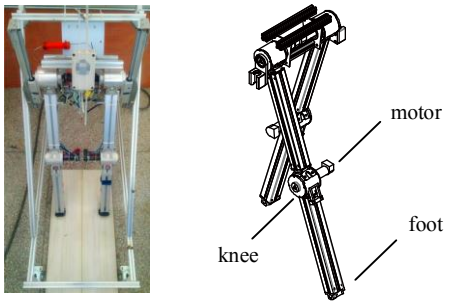


Figure 4. *Robot prototype*

TABLE I. Mass and Length Parameters of the Robot

| Name | Symbol | Numerical Value |
|---|---|---|
| Calf mass/ Thigh mass | $m_c$/$m_t$ | 0.404kg |
| Knee mass | $m_k$ | 0.785kg |
| Motion cage mass | $m_s$ | 5.8kg |
| Hip mass | $m_h$ | 2.537kg |
| Calf length/ Thigh length | $l_c$/$l_t$ | 0.3m |

TABLE II. COMPONENTS USED IN ROBOT

| Name | Model Number | Parameters |
|---|---|---|
| direct current motor | RE25 118752 | power:20W |
| reduction gear box | GP32BZ | reduction ratio: 181:1（hip joint） 236:1（knee joint） |
| encoder | HEDS5540 | number of encoder lines:512 |
| drive | RMDS-102 | precision of control: 13.4mA |
| gyroscope | JY901 | sampling frequency：200Hz |
| pressure sensor | FSR406 | Resistance variation range:0.1KΩ-100 KΩ |
| controller | cRIO9076 | Communication interface: Ethernet port, RS232 serial port |

TABLE III. STIFFNESS COEFFICIENT ( $N/m$ )

| Stiffness | $k_1$ | $k_2$ | $k_3$ | $k_4$ |
|---|---|---|---|---|
| | $10^6$ | $5\times10^5$ | $10^5$ | $10^4$ |

TABLE IV. DAMPING COEFFICIENT ( $N\cdot S/m$ )

| Damping | $c_1$ | $c_2$ | $c_3$ | $c_4$ | $c_5$ |
|---|---|---|---|---|---|
| | $10^6$ | $5\times10^5$ | $10^5$ | $5\times10^4$ | $10^4$ |

TABLE V. WALKING CYCLE AND WALKING SPEED

| | $k_1$ | $k_2$ | $k_3$ | $k_4$ |
|---|---|---|---|---|
| $c_1$ | 10/0.5116 | 10/0.5103 | **11/0.3150** | **11/0.1094** |
| $c_2$ | 11/0.5165 | 11/0.5152 | **11/0.3234** | **4/0.2209** |
| $c_3$ | 11/0.5175 | 11/0.5167 | **11/0.3265** | **1/0.3927** |
| $c_4$ | 10/0.5127 | 11/0.5173 | **11/0.3338** | **1/0.3950** |
| $c_5$ | 7/0.4910 | 6/0.4956 | **12/0.3479** | **2/0.4727** |

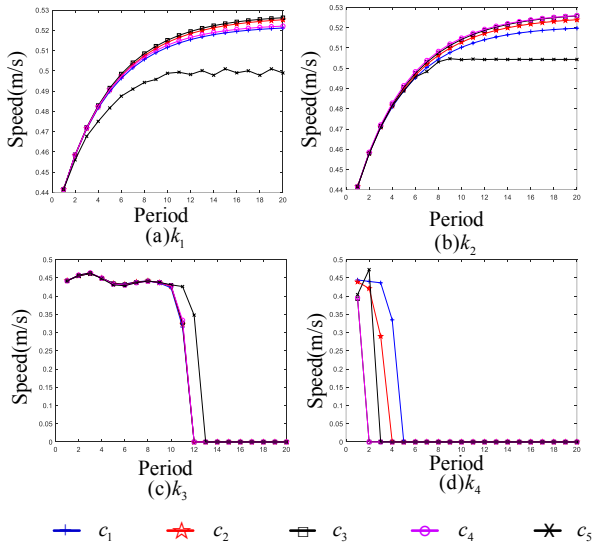


Figure 5. *Walking speed*

The system based on the idea of fast control prototype. The control system includes hardware and software. The main devices used by the prototype are shown in Table II.

Observation of human walking shows that human walking frequency is below 2Hz. In order to achieve stable walking, the sampling frequency should be at least 20 times of the walking cycle. In the system, it takes 5ms for the gyro JY901 to generate data, and the minimum control cycle for the driver to receive instructions is 2ms. The system uses 7ms as the control cycle. The control frequency meets the robot control requirements.

### *B. Robot Walking Simulation*

In order to analyze the stability of the biped robot walking on the ground with different stiffness and damping coefficients, using a compliant ground environment composed of four sets of stiffness coefficients and five sets of damping coefficients as the test environment.

According to the robot structure parameters and initial gait, ensure that the walking can be realized, and the swing foot height is more than 2mm, the specific stiffness and damping coefficient can be seen in Table. III and IV.

Using the coefficients in Table III and Table IV for walking tests, the number of stable or unstable walking cycles $N$ and walking speed $v(m/s)$ can be obtained, as shown in Table V. The bold part in the table is the unstable area, recording the number of cycles and speed when instability occurs, and the rest is the number when entering stable walking.

Under the same stiffness, the walking speed of the robot with different damping coefficients is shown in Fig. 5. By analyzing the data, it can be seen that:

- When the stiffness is $k_1$ and $k_2$, the robot enters the accelerated steady state.
- When the stiffness is $k_3$, the robot enters the unstable state in the 11th or 12th cycle after the control adjustment, the velocity drops to zero.
- When the damping is $c_5$, the robot can enter the stable cycle faster.

### *C. Prototype Experiment*

After the prototype is designed, the walking test is carried out to verify the correctness of the scheme. The control strategy proposed in this paper controls the velocity of the robot's center of mass by adjusting the robot's gait, and finally realizes the underactuated walking.

Firstly, the robot sensor and driver are initialized, and according to the collected initial state $[\,q_i\,,\dot{q}_i\,]^{\mathrm{T}}$ and ideal end state $[\,q_{fd}\,,\dot{q}_{fd}\,]^{\mathrm{T}}$ of the robot walking, the motion trajectory is planned online by using the Bezier curve; After that, the robot joints are tracked and underactuated walking is started; Finally, the controller detects the walking state of the robot. When the support item is switched, the controller plans the trajectory of the next cycle online, and the robot tracks the new trajectory to maintain the underactuated walking. In this paper, the initial state of the robot is collected by the control strategy, and the trajectory is planned online by using the Bezier curve. Compared with the fixed gait, the control strategy can ignore the trajectory tracking error of the previous walking cycle, and the gait of the robot is more natural.

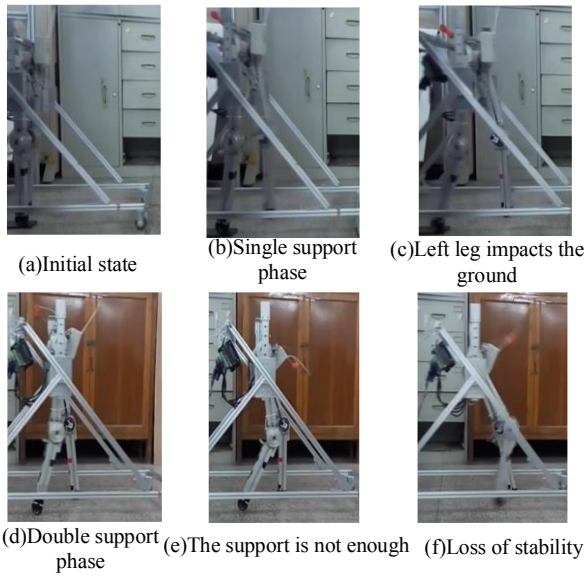


Figure 6. *Concrete floor walking*

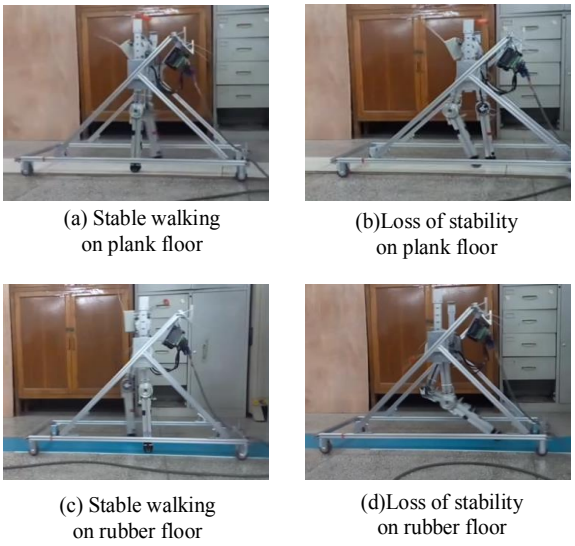


Figure 7. *Plank and rubber floor walking*

Fig. 6 show the walking diagram of the robot on the concrete floor after starting from the vertical plane. Fig. 7 show the robot walking on plank and rubber floor. The walking process of the robot can be divided into four stages:

- The robot starts from the vertical plane, the right leg supports the left leg swing.
- The right leg swings to a certain angle, the left leg contacts the ground. In the next stage, the robot enters the DSP.
- In the DSP, the roles of the swing leg and the support leg are exchanged, the right leg of the robot swings the left leg supports. In the next stage, the robot enters the SSP again.
- The left leg swings to a certain angle, the right leg impacts the ground. The robot enters the DSP.

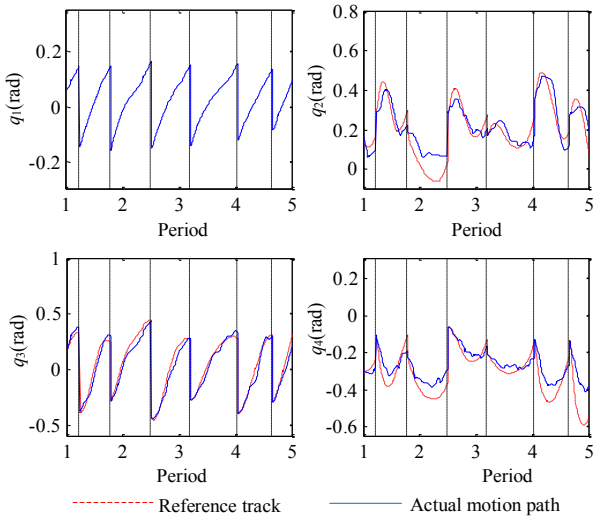


Figure 8. *Robot joint trajectory tracking*

Fig. 8 show the motion trajectory tracking of the robot's underactuated item $q_1$ and active control joints $q_2, q_3$ and $q_4$, with each two dashed lines representing a complete walking cycle. It can be seen from the figure that:

- The underactuated gait has strong robustness, although there are large tracking errors in the walking process (e.g. the $q_2$ and $q_4$ trajectory tracking in the 3rd walking cycle), the robot can still maintain underactuated walking.
- During the walking process, the controller can make online adjustments to the robot's termination gait, since the controller starts working from the 3rd cycle, the termination gait of the first two cycles is the simulated ideal gait.

## V. Conclusion

An adaptive feedforward control strategy is proposed for the stable walking of an underactuated robot in this paper. A prototype of an underactuated biped robot is designed and built. Underactuated walking has strong robustness, and the realization of underactuated walking does not depend on the accurate trajectory tracking control. In this paper, there are still shortcomings in the control strategy, and there is walking instability. The focus of future research is to select a more appropriate control strategy to enable the prototype to walk stably on different compliant grounds.

## References

[1] S. Kuindersma, R. Deits, M. Fallon, et al. "Optimization-based locomotion planning, estimation, and control design for the atlas humanoid robot," *Autonomous Robots*, vol. 40 no. 3, 2016, pp. 429-455.

[2] E. Cerny and J. Gecsei, "The intelligent ASIMO: System overview and integration," presented at the IEEE/RSJ International Conference on Intelligent Robots and Systems, 2002.

[3] M. Fevre, B. Goodwine and J. P. Schmiedeler, "Design and experimental validation of a velocity decomposition-based controller for underactuated planar bipeds," *IEEE Robotics & Automation Letters*, vol. 3, no.3, 2018, pp.1896-1903.

[4] F. Plestan, J. W. Grizzle, E. R. Westervelt, and G. Abba, "Stable walking of a 7-dof biped robot," *IEEE Transactions on Robotics & Automation*, vol. 19, no. 4, 2003, pp. 653–668.
[5] E. R. Westervelt, J. W. Grizzle, C. Chevallereau, J. H. Choi and B. Morris, *Feedback control of dynamic bipedal robot locomotion*. Boca Raton: CRC Press, 2007.
[6] Y. Mao, J. Wang, P. Jia, et al. "A Reinforcement Learning Based Dynamic Walking Control," presented at the IEEE International Conference, on Robotics and Automation (ICRA), Rome, Italy, April,2007.
[7] C. Li, R. Xiong and Q. Zhu, "Push recovery for the standing underactuated bipedal robot using the hip strategy," *Frontiers of Information Technology & Electronic Engineering*, vol. 16, no. 7, pp. 579－593.
[8] P. Zhang, Y. Tian and Z. Liu, "Bisection Method for Evaluation of Attraction Region of Passive Dynamic Walking," presented at the 4th International Conference on Autonomous Robots and Agents (ICARA), Wellington, New Zealand, 2009.
[9] Y. Wang, J. Ding and X. Xiao, "A Position-Domain Adaptive Control Method for Underactuated Bipedal Walking on a Compliant Ground," *International Journal of Humanoid Robotics*, 2019.
[10] D. Yao, Y. Wu, J. He, J. Zhou and X. Xiao, "Feedforward control for underactuated bipedal walking on compliant continuous steps with varying height," *Transactions of the Institute of Measurement and Control*, 2020.
[11] G. Liu, M. Li, W. Guo, and H. Cai, "Control of a biped walking with dynamic balance," presented at the 2012 IEEE International Conference on Mechatronics and Automation, 2012.
[12] D. Yao, S. He, Y. Wu, X. Xiao and Y. Wang, "Feedforward control for underactuated bipedal walking on varying compliant slopes," *Transactions of the Canadian Society for Mechanical Engineering*,2018.
[13] Y. Wang, J. Ding and X. Xiao, "An adaptive feedforward control method for under-actuated bipedal walking on the compliant ground," *International Journal of Robotics and Automation*, 2017.
[14] X. Ni, W. Chen, J. Liu, et al. "A quasi-passive dynamic walker inspired by human walking," *Journal of Central South University (Science and Technology)*, vol. 42, no. 4, 2011, pp. 1028-1034.
[15] C. Chevallereau, J. W. Grizzle and C. L. Shih, "Asymptotically stable walking of a five-link underactuated 3-D bipedal robot," *IEEE Transactions on Robotics*, vol. 25.no. 1, 2009, pp. 37-50.
[16] B. Morris and J. W. Grizzle, "Hybrid Invariant Manifolds in Systems With Impulse Effects With Application to Periodic Locomotion in Bipedal Robots," *IEEE Transactions on Automatic Control*, vol. 54, no. 8, 2009, pp. 1751-1764.
[17] D. Huang, W. Fan, Y. Liu, and T. Liu, "Design of a Humanoid Bipedal Robot Based on Kinematics and Dynamics Analysis of Human Lower Limbs," presented at the IEEE/ASME International Conference on Advanced Intelligent Mechatronics, 2020.
[18] C. Huai and Z. Jin, "Simulation Analysis of Mobile Platform of Grinding Robot Based on Mcnamu Wheel," *Journal of East China Jiaotong University*, vol. 39, no. 5, 2022, pp. 112-119.